Mon. Not. R. Astron. Soc. **000**, 1–?? (2009) Printed 9 November 2010 (MN LATEX style file v2.2)

An analysis of the blue straggler population in the Sgr dSph globular cluster Arp 2⋆

Giovanni Carraro[1]†‡ and Anton F. Seleznev[2]†
[1]*European Southern Observatory, Alonso de Cordova 3107, Casilla 19001, Santiago 19, Chile*
[2]*Astronomical Observatory, Ural State University, Lenin avenue. 51, Ekaterinburg 620083, Russia*

Accepted 2010..... Received 2010...; in original form 2010...

ABSTRACT
We present and discuss new BVI CCD photometry in the field of the globular cluster Arp 2, which is considered a member of the Sagittarius Dwarf Spheroidal Galaxy. The main goal of this investigation is to study of the statistics and spatial distribution of blue straggler stars in the cluster. Blue stragglers are stars observed to be hotter and bluer than other stars with the same luminosity in their environment. As such, they appear to be much younger than the rest of the stellar population. Two main channels have been suggested to produce such stars: (1) collisions between stars in clusters or (2) mass transfer between, or merger of, the components of primordial short-period binaries. The spatial distribution of these stars inside a star cluster, compared with the distribution of stars in different evolutionary stages, can cast light on the most efficient production mechanism at work. In the case of Arp 2, we found that blue straggler stars are significantly more concentrated than main sequence stars, while they show the same degree of concentration as evolved stars (either red giants or horizontal branch stars). Since Arp 2 is not a very concentrated cluster, we suggest that this high central concentration is an indication that blue stragglers are mostly primordial binary stars.

Key words: open clusters and associations: general - open clusters and associations: individual (Arp 2) - binaries: general - blue stragglers - stars: evolution

1 INTRODUCTION

Arp 2 is a globular cluster located at $l = 8.54^o$, $b = -20.78^o$ ($\alpha = 19^h\ 28^m\ 44^s$, $\delta = -30^o21'\ 14''$, J2000.0). It is commonly believed to have formed inside the Sgr dwarf spheroidal galaxy (Monaco et al. 2005), and then released into the Milky Way through tidal interaction. With a metallicity of [Fe/H]=-1.77 (Mottini et al. 2008), this cluster appears to be 3-4 Gyr younger than the old globulars, but $\sim 1-2$ Gyr older than the youngest globulars associated to Sgr (Carraro et al. 2007, Layden & Sarajedini 2000). The first photometric study of this cluster was performed by Buonanno et al. (1994). The derived color-magnitude diagram (CMD) reveals an intriguing feature, namely that the horizontal branch (HB) is located entirely blue-ward of the RR-Lyrae instability strip, a fact that allowed the authors to assess its age through a differential comparison with 47 Tuc and Ruprecht 106. A secondary, prominent feature, which the authors do not comment on, is a group of stars right above the turn-off (TO), which are probably the blue straggler stars (BSS) population in Arp 2. BSS are a normal stellar population in clusters, since they are present in all of the properly observed Globular Clusters (GC, Ferraro 2006; Ferraro et al. 2009, and reference therein). Current scenarios for these stars in globulars are that either they are binary system with significant mass exchange, or stellar mergers resulting from direct collisions between two or more stars (Davies et al. 2004; Knigge et al. 2009; Perets & Frabrycky 2009).

In all these studies a proper assessment of the membership of BSSs through comparison with Red Giant Branch (RGB) stars is routinely performed (Ferraro et al. 1993). The comparison of their cumulative radial distribution may hint to a possible common origin, specifically to confirm or deny whether they belong to the same parent distribution.

Additionaly, the radial distribution of BSS in a star cluster is the most effective tool to understand their origin and which is the dominant production channel (Ferraro 2006). BSS are routinely found - with the exception of Omega Cen and NGC 2419 (Dalessandro et al. 2008)- to be centrally concentrated. Their radial profile then smooths down, while in the cluster periphery it shows again an increase of the BSS contribution (Lanzoni et al. 2007, Dalessandro et al. 2008).

In this paper we report on a new photometric data-set of Arp 2 obtained with the goal of analyzing the BSS population in a young, relatively loose GC, that is in an environment significantly different from a typically dense GC. We anticipate here that our

⋆ Based on observations carried out at ESO La Silla under program 081.C-0087(A).
† On leave from Dipartimento di Astronomia, Universitá di Padova, Italy
‡ E-mail: gcarraro@eso.org (GC); anton.seleznev@usu.ru (AFS)

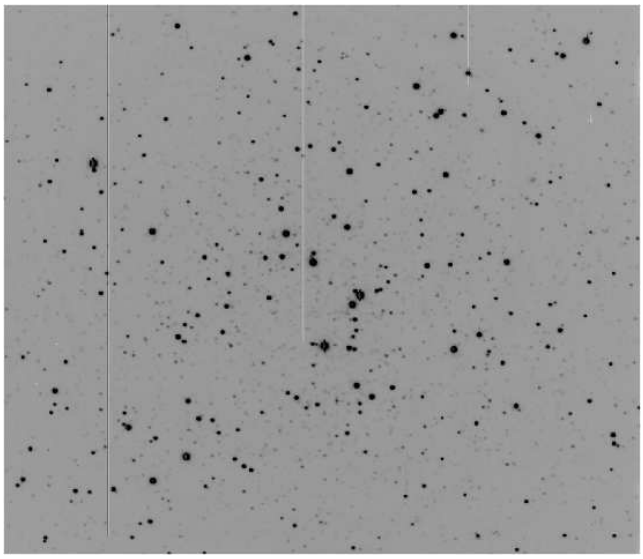

Figure 1. A raw 900 sec image in the I filter of Arp 2. North is up, East to the left, and the field of view if $\sim$ 4 arcmin on a side.

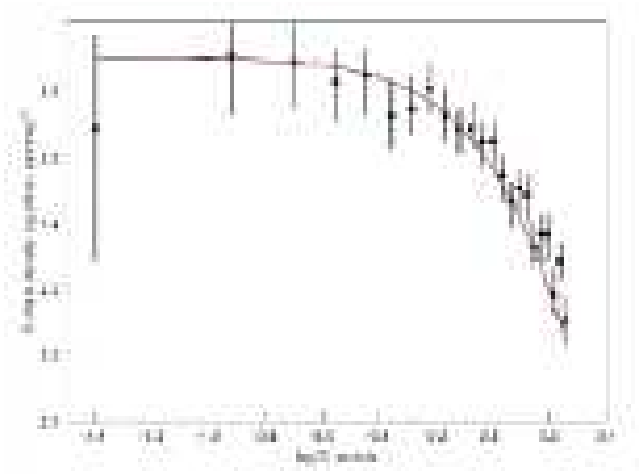

Figure 2. Radial surface density profile as derived from our photometry. Over-imposed is a fit with a King profile, drawn adopting Harrin (1996) parameters

analysis reveals that BSS in Arp 2 do share the same distribution of RGB and horizontal branch (HB) stars, and are more concentrated than main sequence (MS) stars.

This paper is organized as follows. In Sect. 2 we illustrate how we collected and analyzed our data, while in Sect. 3 we present star counts in Arp 2 to measure its size. The CMD of Arp 2 is presented and discussed in Sect. 4, whereas the definition of BSS, and their statistics is discussed in Sect. 6, which, also, comments on and summarizes our findings.

2 OBSERVATIONS AND DATA REDUCTION

CCD BVI images were acquired with the EFOSC2 camera mounted on the Nasmyth focus of the ESO NTT telescope on the night of August 8, 2008. The CCD is a 1030$\times$ 1038 array with a scale of 0.24 arcsec, allowing to cover 4.1$\times$4.1 arcmin on the sky. This allows us to cover a field centered on Arp 2 slightly larger than the previous observations by Buonanno et al. (1994). We used multiple exposures of 30 and 1200 secs for the B filter, and 30 and 900 both for V and I filters. As an illustration, an I filter, 900 sec, raw image is shown in Fig. 1. The night was photometric, and we calibrated our photometry against the Landolt (1992) standard field Mark A and PG 2213, observed several times during the night. Arp 2 was observed during an observational run focused on a different science when the principal target was not visible. Data have been reduced in the standard way. Image preparation (trimming, bias and flatfield) was done using the IRAF package, while photometry was extracted by using DAOPHOT and ALLSTAR (Stetson 1987). We obtained a final catalog with 4580 entries having 2000.0 Equatorial coordinates, and B, V and I magnitudes together with associated uncertainties. These latter have been calculated following the prescriptions described in Patat & Carraro (2001).

2.1 Complementary infrared data, astrometry and completeness

Our optical catalogue was cross-correlated with 2MASS, which resulted in a final catalog including BVI and JHK_s magnitudes. As a by product, pixel (detector) coordinates were converted to RA and DEC for J2000.0 equinox, thus providing 2MASS-based astrometry.

Finally, completeness corrections were determined by running artificial star experiments on the data. The data-set was divided in two regions, inner (inside 1 arcmin) and outer (beyond 1 arcmin), and completeness was computed for these two different regions, which, due to the nature of the object, are expected to be differently affected by star crowding (Carraro et al. 2007). Basically, we created several artificial images by adding artificial stars to the original frames. These stars were added at random positions, and had the same color and luminosity distribution of the true sample. To avoid generating overcrowding, in each experiment we added up to 30% of the original number of stars. Depending on the frame (short or deep exposures), between 1000-5000 stars were added. In this way we have estimated that the completeness level of our photometry in the outer region is 100% down to V = 23.00, and better than 50% down to V = 23.50. As for the inner region, we found that the completeness is 100% down to V = 22.40, and better than 50% down to V = 22.80.

3 STAR COUNTS AND CLUSTER SIZE

We used our photometry to study the cluster stars radial distribution. According to Harris (1996), Arp 2 has a concentration c=0.90, an half-mass radius = 1.91 arcmin, and a core and tidal radius of 1.59 and 12.65 arcmin, respectively. Therefore we expect our photometry to cover just the inner part of the cluster. The radial density profile we constructed is shown in Fig. 2. It has been derived following the method described in Seleznev (1994). This method employs numerical differentiation of the best mean-square polynomial fit for N(r), the number of stars in circles of radius r in the plane of the sky. The center of the cluster was taken at the detector coordinates (512,512) which corresponds to $\alpha = 19^h\ 28^m\ 44^s$, $\delta = -30^o21'\ 14''$ (J2000.0). Vertical bars indicate the profile errorbars derived assuming Poisson statistics. In the same Fig. 2 we fit the profile with a King (1962) model, adopting king parameters (core and tidal radius, and center mass density) from Harris (1996)

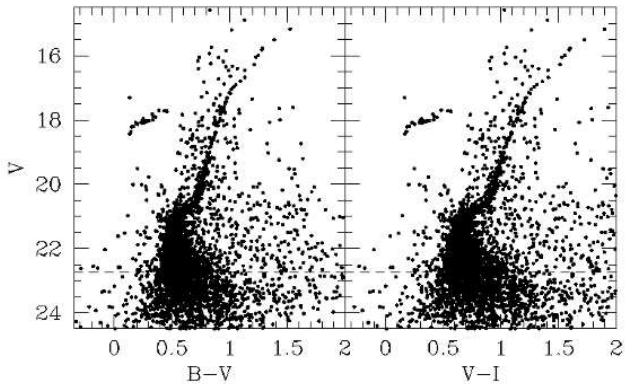

Figure 3. CMD in the V vs B-V (left panel), and V vs V-I (right panel) for Arp 2. The dashed lines indicate the 100% level of completeness. See Sect. 2.1

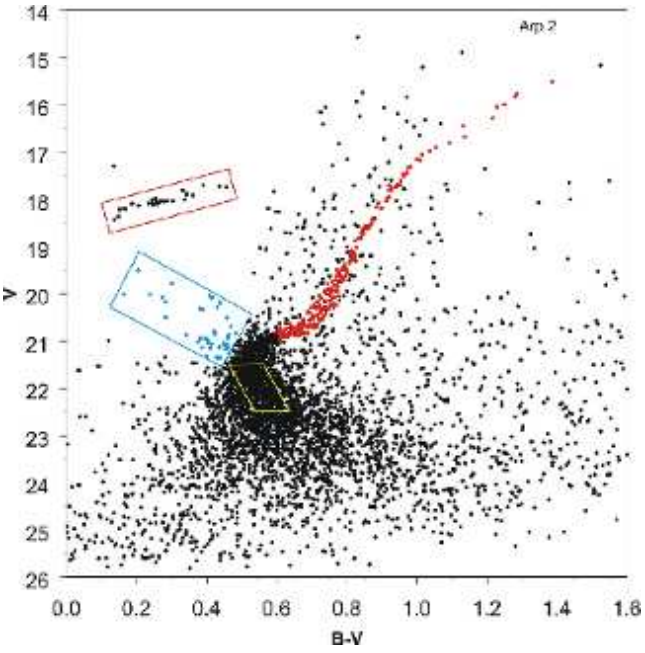

Figure 4. Selection of RGB (red dots), HB (red circle), BSS (cyan circle) and MS (yellow polygon) stars. These latter have been selected in a region of the MS where the completeness is 100%.

compilation. The fit is good within the uncertainties, and therefore we conclude that Arp 2 follows a King-like density profile. It decreases all the way to the edge of the field we covered, slightly beyond the nominal half-mass radius.

4 COLOR MAGNITUDE DIAGRAMS

The resulting color magnitude diagrams (CMDs) are shown in the two panels of Fig. 3. In the left panel, the V versus B-V diagram is shown, while in the right panel we present the V versus V-I. The CMD on the left panel is absolutely identical to the one presented by Buonanno et al.(1994), apart from the slightly different area coverage and the magnitude limit, which in our case is about one magnitude fainter. All the typical features of a globular cluster CMD are present. The MS, RGB, HB -located entirely blue-ward the RR Lyrae instability strip-, and the Asimptotic Giant Branch (AGB). An additional feature which has been overlooked in the past is the plume of blue stars right above the turn off point (TO), which is quite common in globular clusters, and it is composed of candidate blue straggler stars. This plume is the target of our investigation. We look for BSS candidates following the commonly used criteria (Ahumada & Lapasset 1995, 2007; Sandage 1953), which is illustrated in Fig. 4. Together with BSS (blue box), we also indicated the location of HB (red box), RGB (red dots), and a sample of MS stars (yellow box), which we are going to compare. We counted 41 BSS candidates, and 28 HB stars. They are listed in Table 1 and 2, respectively, where we indicate stars' identification (our numbering, ID), equatorial coordinates for the 2000.0 equinox, magnitude V and color B-V. These can also be useful for future spectro-scopic follow-up.
Besides, again following Fig 4, we counted 213 RGB and 517 MS stars, which we do not list here for space reasons. As for MS stars, we stress that they have been extracted in a region of the MS which is not affected by incompleteness.

We stress that the numbers we reported have been computed using the classical definition of BSS locus and assuming that contamination from field stars is negligible, which seems to be the case, since the field of view is very small (0.0044 squared degrees). However, we do not have at our disposal a control field to verify this directly. Therefore, we investigated the amount of contamination by computing synthetic CMDs of stars in the direction of Arp 2 assuming a Galactic model which includes bulge, halo, thin and thick disks (Girardi et a. 2005). We generated several CMDs by varying the random seed and added photometric errors as from Arp 2 photometry. The results are shown in Fig. 5, where the left panel shows the Galaxy CMD in the direction of Arp 2, and the right panel the CMD of Arp 2 as in Fig. 4. In both panel we indicate the boxes used for selecting HB (red) and BSS (blue) stars. A quick glance at this figure is sufficient to conclude that most of the contamination affects the lower MS, and in general contaminating stars are redder than the typical BSS colors. Some contamination is present in the RGB area but, provided the high number of RGB stars in Arp 2, we do not expect their statistics to be significantly affected.

5 ANALYSIS OF THE BLUE STRAGGLER STARS' POPULATION

To properly assess the probable membership of BSS, it is necessary to measure their radial velocity or their proper motion (Mathieu & Geller 2009; Liu et al. 2008). Since we are relying only on photometry, we will keep considering our BSS as candidates, based on their location in the CMD. To get more insight on their properties and origin, we started by considering their surface distribution, and compared it with the surface distribution of HB stars. This is illustrated in Fig 6, which shows radial density profile of the two populations. Here we plot the number of stars per squared arcmin as computed in concentric bins 10 arcsecs wide. Except for the difference in the inner side of the cluster, the two profiles are identical. We stress that the difference in the very central bin, although real, is exagerated by the small number statistics (2 BSS and 0 HB stars). In this respect Arp 2 seems more similar to old open clusters, like M 67 (Mathieu & Gheller 2009), than to genuine globulars. The higher concentration of BSS in the cluster internal region with respect to evolved stars we find is not new, and has been found already in several other globulars (Dalessandro et al 2008). At odds

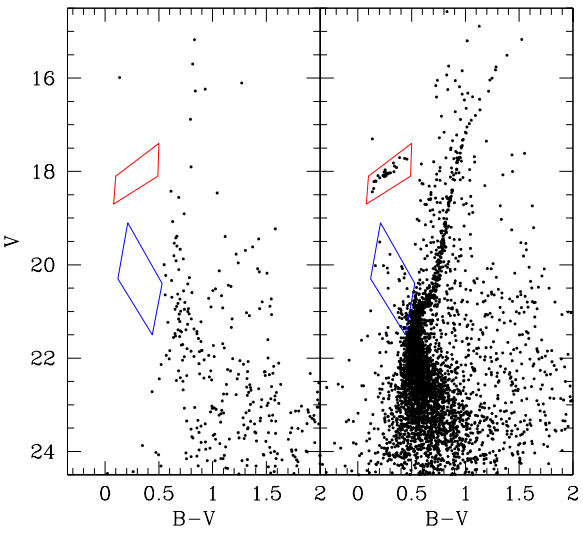

Figure 5. Estimate of field star contamination in Arp 2. The left panel shows the Galaxy CMD in Arp 2 direction, and the right panel the CMD of Arp 2 as in Fig. 4.

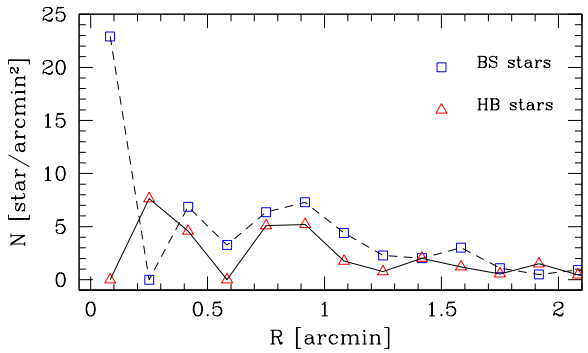

Figure 6. Radial surface density profile of HB (red triangles) and BSS (blue squares) stars i n the field of Arp 2

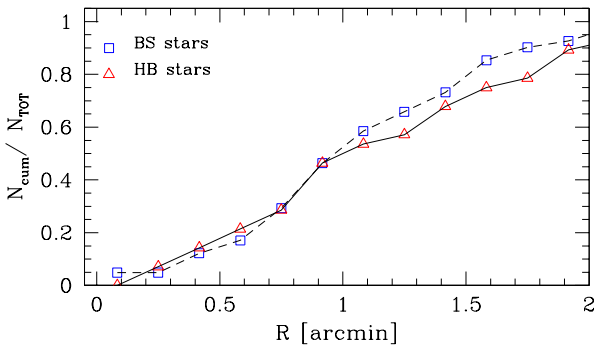

Figure 7. Fractional radial cumulative distribution of BSS and HB stars

Table 1. BSS candidates. See Fig. 4 for the selection

ID	$\alpha(2000.0)$	$\delta(2000.0)$	V	B-V
140	292.1463587	-30.3394516	19.777	0.299
742	292.1539322	-30.3574441	21.321	0.400
909	292.1560467	-30.3590792	20.831	0.482
1086	292.1584272	-30.3590217	21.173	0.453
1119	292.1590122	-30.3404261	20.071	0.274
1463	292.1627267	-30.3544101	20.191	0.437
1575	292.1639108	-30.3676803	21.347	0.438
1649	292.1649792	-30.3565927	21.040	0.448
1942	292.1681176	-30.3770277	20.871	0.340
2257	292.1718385	-30.3564573	20.680	0.469
2308	292.1723293	-30.3570290	20.282	0.430
2324	292.1727334	-30.3409102	20.315	0.382
2341	292.1725939	-30.3588043	21.154	0.410
2433	292.1741541	-30.3208680	20.853	0.423
2531	292.1743077	-30.3790334	21.371	0.431
2568	292.1748233	-30.3722961	21.268	0.462
2750	292.1770090	-30.3470938	21.341	0.430
2826	292.1779222	-30.3386991	21.040	0.403
2910	292.1782726	-30.3795017	21.024	0.374
2913	292.1788245	-30.3432700	20.935	0.460
3146	292.1810024	-30.3573719	20.947	0.396
3163	292.1815525	-30.3322570	20.343	0.388
3266	292.1822050	-30.3519277	21.131	0.386
3351	292.1829014	-30.3662331	20.172	0.281
3362	292.1830748	-30.3598515	20.039	0.408
3533	292.1851738	-30.3394198	20.981	0.402
3633	292.1858386	-30.3652012	20.082	0.414
3637	292.1860246	-30.3541686	21.078	0.458
4014	292.1899276	-30.3349827	20.018	0.163
4140	292.1907422	-30.3659681	20.510	0.458
4346	292.1932713	-30.3685683	20.874	0.462
4420	292.1946120	-30.3279961	21.127	0.435
4635	292.1967567	-30.3540156	19.512	0.203
4875	292.1993316	-30.3591077	21.066	0.413
5059	292.2014691	-30.3478313	22.921	0.668
5174	292.2029316	-30.3524965	20.789	0.421
5239	292.2037376	-30.3534943	20.504	0.282
5354	292.2051005	-30.3629483	21.345	0.428
5611	292.2091052	-30.3263457	20.941	0.382
5612	292.2085462	-30.3696267	21.149	0.460
6087	292.2157226	-30.3813623	20.019	0.238

with what is found in other globulars, we do not see any outward increase of the BSS population, most probably because we are not sampling the cluster outskirts (see Section 3)in this study .

6 DISCUSSION AND CONCLUSION

To better quantify the relationship between BSS and the other stars we make use of Kolmogorov-Smirnov (KS) statistics, in its one (1D) and two (2D) dimensional flavors.

The 2D distributions of BSS with respect to other star samples in different evolutionary phases (HB, RGB or MS stars) were statistically compared with the 2D generalization of 1D KS test described in Press et al. (1997) and Fasano & Francheschini (1987). The same method was employed in Pancino et al. (2003) for comparison of the 2D distributions of RGB stars with different metallicity in the multi-population globular cluster ω Cen.

This test gives the probability P that two distributions are extracted

Table 2. HB candidates. See Fig. 4 for the selection

ID	$\alpha(2000.0)$	$\delta(2000.0)$	V	B-V
125	292.1456946	-30.3733031	17.819	0.331
370	292.1493758	-30.3477929	18.091	0.260
1127	292.1586924	-30.3658908	18.069	0.254
1549	292.1641508	-30.3352455	17.735	0.456
1996	292.1690971	-30.3519957	18.139	0.204
2040	292.1691049	-30.3828881	18.207	0.162
2086	292.1701074	-30.3484238	17.966	0.253
2503	292.1746582	-30.3377476	18.087	0.256
2608	292.1753085	-30.3659882	18.219	0.150
3036	292.1802420	-30.3302122	18.007	0.336
3038	292.1802864	-30.3280083	18.367	0.147
3129	292.1807069	-30.3656050	18.089	0.186
3204	292.1815674	-30.3589202	18.038	0.271
3555	292.1848119	-30.3832435	18.087	0.234
3682	292.1864725	-30.3582211	17.996	0.253
3772	292.1871954	-30.3651926	17.886	0.341
3990	292.1894482	-30.3534246	17.703	0.388
4040	292.1898984	-30.3533154	17.917	0.360
4911	292.1998576	-30.3476994	18.097	0.258
4932	292.2002557	-30.3352233	17.720	0.435
4940	292.1997888	-30.3748761	18.209	0.168
5048	292.2011579	-30.3552338	18.054	0.277
5101	292.2019892	-30.3501858	18.437	0.135
5165	292.2033021	-30.3208588	18.108	0.245
5184	292.2029381	-30.3599449	18.018	0.243
5244	292.2038283	-30.3544071	18.028	0.304
5646	292.2087883	-30.3863411	18.051	0.266
5773	292.2115368	-30.3289674	18.037	0.287

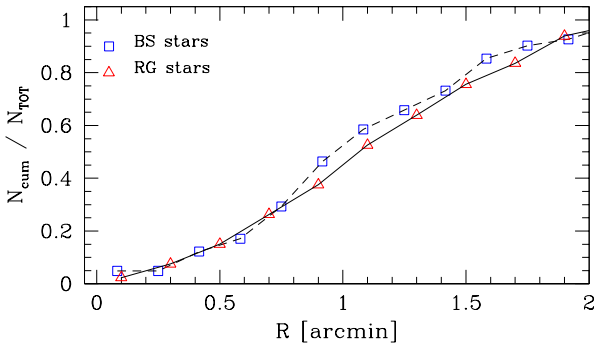

Figure 8. Fractional radial cumulative distribution of BSS and RGB stars

from the same parent distribution. Small values of P would show that the two samples are significantly different. Formulas as given in Press et al. (1997) are accurate enough when

$$N = N_1 \cdot N_2/(N_1 + N_2) > 20 \quad (1)$$

and when the indicated probability P is less (more significant than) 0.20 or so. In the above equation N1 and N2 are the two populations under comparison. When P is larger than 0.20, its value may not be accurate, but the implication that the two data sets are not significantly different is certainly correct. We summarize our results in Table 3 and 4, and graphically in the series of Figs. 7 to 9.
Looking at the results listed in the two tables and illustrated in the corresponding figures, we can provide the following considerations.

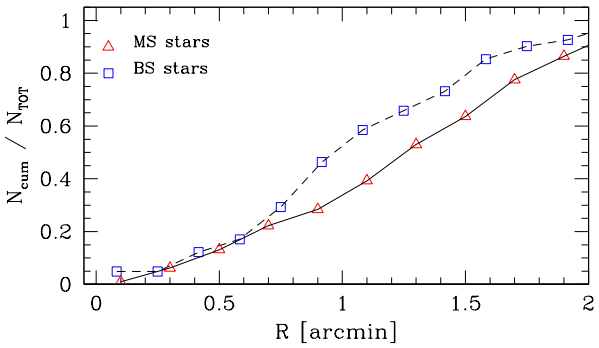

Figure 9. Fractional radial cumulative distribution of BSS and MS stars

Table 3. Results of the KS statistics in 1D for the BSS.

Population	N	P	Reference Figure
HB	17	0.83	Fig 7
RGB	35	0.61	Fig 8
MS	38	0.07	Fig 9

First, due to the larger number, the statistics (N) improves passing from HB to RGB stars, and from RGB to MS stars.

Second, probabilities P for 2D KS test are smaller than for 1D test in the case of HB and RGB stars. We face the opposite situation as for MS stars. We can explain it by taking into account that 1D distribution is only a function of the distance from the distribution center, while 2D distributions do contain angle information. In the case of HB and RGB stars radial distributions are very close to BSS, while azimuthal distributions have some differences, and this results in larger probabilities in 1D testing. In the case of MS stars radial distribution is very different from BSS distribution, and probability in 1D test is small. Apparently, azimuthal distributions in this case are more similar, which implies larger probability in 2D test.

Third, and more interesting, the tests provide comparable results for HB and RGB stars. This implies that BSS, HB and RGB stars are on the overall distributed in the same way, which in turn means that these populations are not significantly different. We caution however that high probability in KS test is a necessary, but not sufficient condition to prove that these populations have the same parent distribution (see e.g. Press et al., 1997).

At odds with HB and RGB, MS stars show a different distri-

Table 4. Results of the KS statistics in 2D for the BSS.

Population	N	P
HB	17	0.51
RGB	35	0.43
MS	38	0.23

bution when compared to BSS. Namely, BSS are significantly more concentrated to the cluster center than normal MS stars. All-together this suggests that most probably BSS are primordial binary systems which, because of their total mass and the relatively loose environment of Arp 2, sank toward the center and survived as binary system.

Our results also imply that present-day RGB and HB stars are, on the overall, more concentrated than actual MS stars. This does not mean that actual HB stars and upper RGB stars are more massive than actual MS stars, which can be the case for RGB stars in earlier stages of evolution. This simply reflects the fact that actual upper RGB and HB stars follow the spatial distribution of their -originally more massive- MS progenitors. The relaxation time for Arp 2 is $\sim$5 Gyr (Harris 1996), specifically much shorter than the cluster age, and therefore mass segregation already occured in the past, when the progenitors of present-day upper RGB and HB stars were in the MS, and were more massive - and therefore more segregated - than the present-day MS stars.

Our findings confirm very recent results on the BSS distribution and nature in GCs (Ferraro et al. 2009).
The suggestions (Knigge et al. 2009) that most BSS in globulars have a binary origin, even in the environment of the densest globulars, is not longer of general validity. In fact, whether BSS are primordial close binaries or merger remnants resulting from direct collision between two stars, depends strongly on the environment. As recently discovered by Ferraro et al. (2009), the existence of double BSS sequences in M30, a famous *core collapse* globular cluster, confirms that BSS nature depends strongly on the environment, and the dynamical state of the parent cluster.
Loose systems, such as open clusters, do indeed show a high primordial binary fraction among their BSS (Mathieu & Gheller 2009), while very dense systems harbour both primordial binaries and merger products, in proportions which vary from cluster to cluster.

In this context, Arp 2 is a relatively low concentration globular, that follows this trend, which will be hopefully confirmed by future spectroscopic observations.

ACKNOWLEDGMENTS

GC expresses his gratitude to O. Hainaut and G. Lo Curto for assistance during the observations, and Y. Momany for long useful conversations on blue stragglers. We express special thanks to the referee, Robert Rood, for the careful reading and useful suggestions he provided. Finally, we expresse our gratitude to Sandy Strunk for reading carefully the manuscript and improving the language. In preparation of this paper, we made use of the NASA Astrophysics Data System and the ASTRO-PH e-print server. This work made extensive use of the SIMBAD database, operated at the CDS, Strasbourg, France.

REFERENCES

Ahumada, J.A., Lapasset, E., 1995, A&A 109, 375
Ahumada, J.A., Lapasset, E., 2007, A&A 463, 789
Buonanno, R., Corsi, C.E., Fusi Pecci, F., Fahlman, G.G., Richer, H.B., 1994, ApJ, 430, L121
Carraro, G., Zinn, R., Moni Bidin, C., 2007, A&A, 466, 181
Dalessandro, E., Lanzoni, B., Ferraro, F. R., Vesperini, F., Bellazzini, M., Rood, R. T. 2008, ApJ, 681, 311
Dalessandro, E., Lanzoni, B., Ferraro, F.R., Rood, R.T., Milone, A., Piotto, G., Valenti, E., 2008, ApJ, 677, 1069
Davies, M., Piotto, G., de Angeli, F., 2004, MNRAS, 349, 129
Fasano, G., Franceschini, A., 1987, MNRAS, 225, 155
Ferraro, F.R., Fusi Pecci, F., Cacciari, C., Corsi, C, Buonanno, R., Fahlam, G.G., Richer, H.B., 1993, AJ, 106, 2324
Ferraro, F., 2006,in Modelling Dense Stellar Systems, 26th meeting of the IAU, JD14, 4
Ferraro, F.R., Beccari, G., Dalessandro, E., Lanzoni, B., Sills, A., Rood, R.T., Fusi Pecci, F., Karakas, A.I., Miocchi, P., Bovinelli, S., 2009, Nature, 462, 24
Girardi L.,Groenewegen, M. A. T., Hatziminaoglou, E., da Costa, L. 2005, A&A, 436, 895
Harris, W.E., 1996, AJ, 112, 1487
Knigge, C., Leigh, N.,Sills, A., 2009, Nature, 457, 15
Layden, A.C., Sarajedini, A., 2000, AJ 119, 1760
Landolt, A.U, 1992, AJ, 104, 372
Lanzoni, B., Dalessandro, E., Ferraro, F.R., Mancini, C., Beccari, G., Rood, R.T., Mapelli, M., Sigurdsson, S., 2007, ApJ, 663, 267
Liu, G.Q., Deng, L., Chávez, M., Bertone, E., Herreo Davo, A., Mata-Chávez, M.D., 2008, MNRAS, 390, 665
Mathieu, R.D., Gheller, A.M., 2009, Nature, 462, 24
Monaco, L., Bellazzini, M., Bonifacio, P., Ferraro, F.R.,Marconi, G., Pancino, E., Sbordone, L., Zaggia, S., 2005, A&A, 441, 141
Mottini. M., Wallerstein, G., McWilliam, A., 2008, AJ, 136, 614
Pancino, E., Seleznev, A., Ferraro, F.R., Bellazzini, M., Piotto, G., 2003, MNRAS, 345, 683
Patat, F., Carraro, G., 2001, MNRAS 325, 1591
Perets, H.B., Fabrycky, D.C., 2009, ApJ 697, 1048
Press, W.H., Teukolsky, S.A., Vetterling, W.T., Flannery, B.P, 1997, Numerical Recipes of Fortran 77. The Art of Scientific Computing, 2nd edn. Cambridge Univ. Press, New York.
Sandage, A.R., 1953, AJ, 58, 61
Sandquist, E.L. 2005, ApJ, 635, L73
Seleznev, A.F., 1994, A&Ap Trans, 4, 167
Stetson, P.B., 1987, PASP, 99, 191